

Saturation and Geometrical Scaling: from Deep Inelastic ep Scattering to Heavy Ion Collisions *

MICHAŁ PRASZALOWICZ

M. Smoluchowski Institute of Physics, Jagiellonian University,
ul. S. Łojasiewicza 11, 30-348 Kraków, Poland.

Saturation of gluon distribution is a consequence of the non-linear evolution equations of QCD. Saturation implies the existence of so called saturation momentum which is defined as a gluon density per unit rapidity per transverse area. At large energies for certain kinematical domains saturation momentum is the only scale for physical processes. As a consequence different observables exhibit geometrical scaling (GS). We discuss a number of examples of GS in different reactions.

PACS numbers: 13.85.Ni,12.38.Lg

1. Introduction

At the eQCD meeting in 2013 [1] we have discussed the emergence of geometrical scaling [2] for F_2/Q^2 in deep inelastic scattering (DIS) [3] and for charged particle distributions in proton collisions [4]. Here, after short reminder, we extend this analysis to $\langle p_T \rangle (N_{ch})$ correlation [5, 6] and to heavy ion collisions (HI) [7]. References [1], [3]–[7] include a more complete bibliography of the subject.

Geometrical scaling hypothesis means that some observable σ that in principle depends on two independent kinematical variables, say x and Q^2 , in fact depends only on a specific combination of them denoted as τ :

$$\sigma(x, Q^2) = S_{\perp} F(\tau). \quad (1)$$

Here function F in Eq. (1) is a dimensionless function of scaling variable

$$\tau = Q^2/Q_s^2(x). \quad (2)$$

* Presented at the Conference *Excited QCD*, Taranska Lomnica, Slovakia, March 8 – 14, 2015.

and

$$Q_s^2(x) = Q_0^2 (x/x_0)^{-\lambda} \quad (3)$$

is the saturation scale. S_{\perp} is a transverse area that corresponds to the overlap of hadrons colliding at fixed impact parameter b (or integrated over db), or – like in the case of DIS – it is a cross section for large dipole scattering on a proton. Q_0 and x_0 in Eq. (3) are free parameters, which can be extracted from the data within some specific model for σ , and parameter λ is a dynamical quantity of the order of $\lambda \sim 0.3$. Here we shall test the hypothesis whether different pieces of data can be described by formula (1) with *constant* λ , and what is the range of transverse momenta where GS is working satisfactorily. Throughout this paper we shall be neglecting logarithmic energy dependence due to the running of α_s .

2. Deep Inelastic Scattering at HERA

Let us start with DIS where the relevant scaling observable is $F_2(x)/Q^2$ [2]. In Fig. 1 we plot $F_2(x)/Q^2$ as a function of Q^2 (left panel) and in terms of τ for $\lambda = 0.329$ (right panel) for combined HERA data [8]. Different points correspond to different Bjorken x 's. We see from Fig. 1 that points of different Bjorken x 's scale very well with some exception in the right part of Fig. 1.b. These points, however, correspond to large Bjorken x 's where GS is supposed to break.

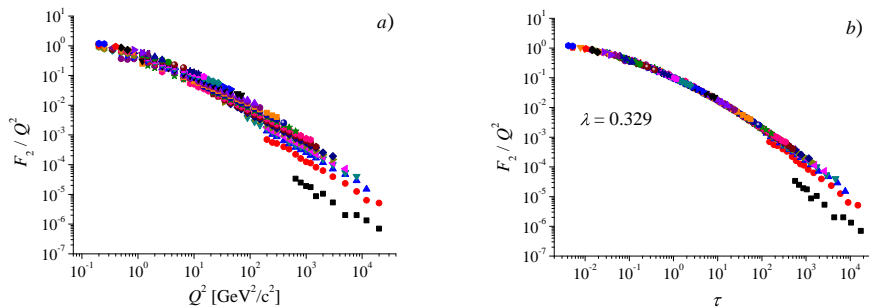


Fig. 1. Combined DIS data [8] for F_2/Q^2 . Different points forming a wide band as a function of Q^2 in the left panel correspond to different Bjorken x 's. They fall on a universal curve when plotted in terms of τ (right panel). (Figure from the first paper of Ref. [3]).

3. Inelastic p_T spectra at the LHC

In hadronic collisions at c.m. energy $W = \sqrt{s}$ particles are produced in the scattering process of two patrons characterized by Bjorken x 's

$$x_{1,2} = e^{\pm y} p_T/W. \quad (4)$$

For central rapidities $x = x_1 \sim x_2$. Geometrical scaling in this case means simply that [4]:

$$\left. \frac{dN}{dy d^2 p_T} \right|_{y \simeq 0} = S_{\perp} F(\tau) \quad (5)$$

where F is a universal dimensionless function of the scaling variable

$$\tau = p_T^2/Q_s^2(x) = p_T^2/Q_0^2 (p_T/(x_0 W))^{\lambda}. \quad (6)$$

In Fig. 2 we plot ALICE pp data [9] in terms of p_T (left panel) and in terms of scaling variable τ (right panel) for $\lambda = 0.22$. We have found by a model independent analysis that the optimal exponent $\lambda = 0.22 - 0.24$ [10], which is smaller than in the case of DIS. Why this so, remains to be understood.

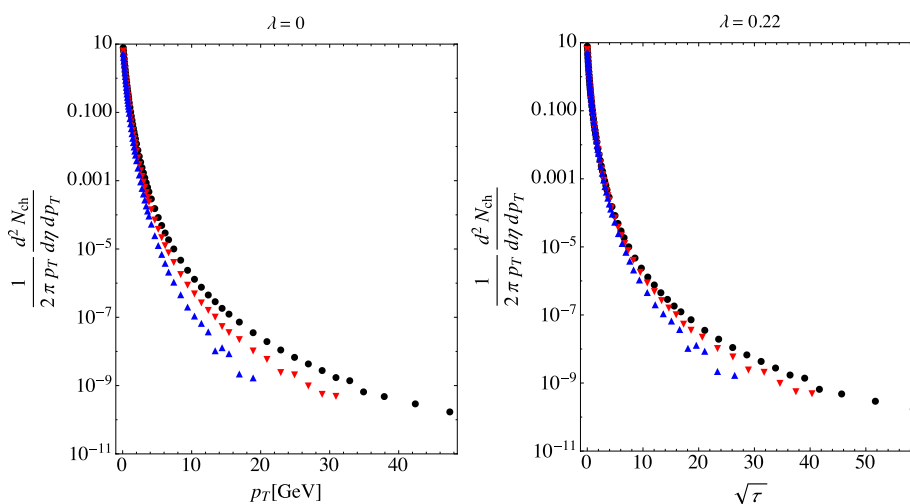


Fig. 2. Data for pp scattering from ALICE [9] plotted in terms of p_T and $\sqrt{\tau}$. Full (black) circles correspond to $W = 7$ TeV, down (red) triangles to 2.76 TeV and up (blue) triangles to 0.9 TeV.

An immediate consequence of GS for the p_T spectra is a power-like growth of multiplicity with energy. Indeed, since

$$p_T = \bar{Q}_s(W)\tau^{1/(2+\lambda)} \quad (7)$$

where the *average* saturation scale is defined as

$$\bar{Q}_s(W) = Q_0 (x_0 W/Q_0)^{\lambda/(2+\lambda)} \quad (8)$$

one arrives at

$$\frac{dN}{dy} = S_{\perp} \bar{Q}_s^2(W) \times \left[\frac{1}{2+\lambda} \int \mathcal{F}(\tau) \tau^{2/(2+\lambda)} \frac{d\tau}{\tau} \right]. \quad (9)$$

Data indeed support the power-like growth of inelastic multiplicity as $s^{0.1}$ as predicted by GS by Eq. (8) for $\lambda = 0.22 - 0.24$.

4. Mean p_T in hadronic collisions at the LHC

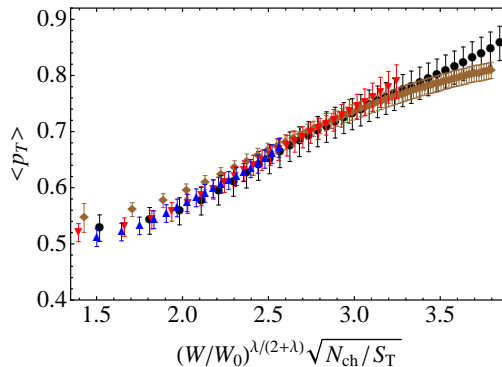


Fig. 3. Mean $\langle p_T \rangle$ in pp collisions at 7 TeV (full black circles), 2.76 TeV (full red down-triangles), 0.9 TeV (full blue up-triangles) and in pPb collisions at 5.02 TeV (full brown diamonds) plotted in terms of scaling variable $(W/W_0)^{\lambda/(2+\lambda)} \sqrt{N_{ch}/S_T}$. For pp $W_0 = 7$ TeV and for pPb $W_0 = 5.02$ TeV. (Figure from the second paper of Ref. [5].)

Another consequence of Eq. (5) is that [5]

$$\langle p_T \rangle \sim \bar{Q}_s(W), \quad (10)$$

which means that $\langle p_T \rangle$ rises with energy as $W^{\lambda/(2+\lambda)}$, which is indeed seen in the data. On the other hand, since the saturation momentum is by Eq. (8) equal to the gluon density per transverse area, one easily derive

the correlation between mean p_T and charged particles multiplicity at given energy W [5]:

$$\langle p_T \rangle|_W \sim \left(\frac{W}{W_0} \right)^{\lambda/(2+\lambda)} \sqrt{\frac{N_{\text{ch}}}{S_{\perp}(N_{\text{ch}})|_{W_0}}}. \quad (11)$$

By fixing multiplicity, one is probing some fixed impact parameter that corresponds to the overlap transverse area $S_{\perp}(N_{\text{ch}})$ that itself is by construction both multiplicity and energy dependent. Therefore one needs a model for $S_{\perp}(N_{\text{ch}})$. To this end we have used the Color Glass Condensate result for pp and pA collisions [11]. The result is plotted in Fig. 3 where we plot ALICE data [12] as a function of scaling variable defined in Eq. (11)

5. Geometrical Scaling in heavy ion collisions

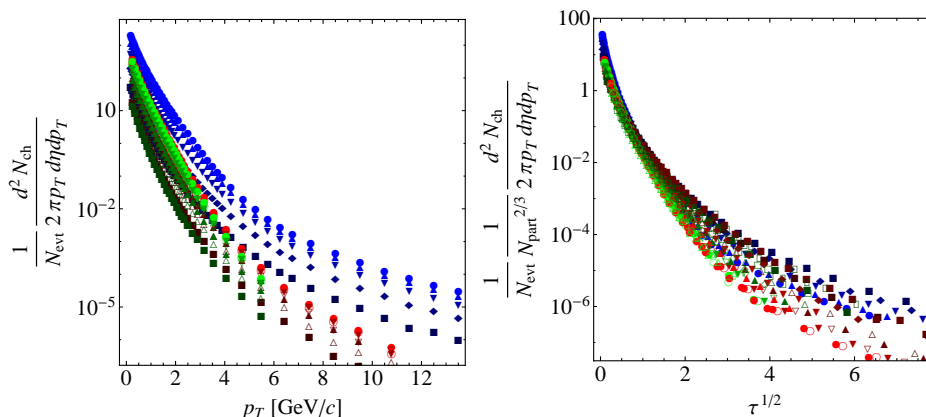


Fig. 4. Illustration of geometrical scaling in heavy ion collisions at different energies and different centrality classes. Left panel shows charged particle distributions from ALICE [15], STAR [16, 17] and PHENIX [18, 19] plotted as functions of p_T . In the right panel the same distributions are scaled according to Eq. (13).

GS for particle spectra in HI collisions has been already discussed in Ref. [7] and in Ref. [13] for photons. HI data are divided into centrality classes that select events within certain range of impact parameter b . In this case both transverse area S_{\perp} and the saturation scale Q_s^2 acquire additional dependence on centrality that is characterized by an average number of participants N_{part} . We have [13, 14]:

$$S_{\perp} \sim N_{\text{part}}^{2/3} \text{ and } Q_s^2 \sim N_{\text{part}}^{1/3}. \quad (12)$$

Therefore in HI collisions

$$\frac{1}{N_{\text{evt}}} \frac{dN_{\text{ch}}}{N_{\text{part}}^{2/3} d\eta d^2p_{\text{T}}} = \frac{1}{Q_0^2} F(\tau) \quad \text{where} \quad \tau = \frac{p_{\text{T}}^2}{N_{\text{part}}^{1/3} Q_0^2} \left(\frac{p_{\text{T}}}{W} \right)^\lambda. \quad (13)$$

In Fig. 4 we plot LHC and RHIC data in terms of p_{T} (left panel) and $\sqrt{\tau}$ for $\lambda = 0.3$ (right panel). One can see an approximate scaling of, however, worse quality than in the pp case.

To summarize: a wealth of data in hadronic collisions exhibit GS. This may be interpreted as a signature of saturation. However some details, like the non-universality of the value of λ , remain to be understood.

This work was supported by the Polish NCN grant 2014/13/B/ST2/02486.

REFERENCES

- [1] M. Praszalowicz, *Acta Phys. Polon. Supp.* **6** (2013) 809.
- [2] A. Stasto, K. Golec-Biernat, J. Kwiecinski, *Phys. Rev. Lett.* **86** (2001) 596.
- [3] M. Praszalowicz, T. Stebel, *JHEP* **1303** (2013) 090 and *JHEP* **1304** (2013) 169.
- [4] L. McLerran, M. Praszalowicz, *Acta Phys. Polon. B* **41** (2010) 1917, and *Acta Phys. Polon. B* **42** (2011) 99.
- [5] L. McLerran, M. Praszalowicz, B. Schenke, *Nucl. Phys. A* **916** (2013) 210 and L. McLerran, M. Praszalowicz, *Phys. Lett. B* **741** (2015) 246.
- [6] M. Praszalowicz, *AIP Conf. Proc.* **1654** (2015) 080001.
- [7] M. Praszalowicz, *Acta Phys. Polon. B* **42** (2011) 1557 and arXiv:1205.4538 [hep-ph].
- [8] C. Adloff *et al.* [H1], *Eur. Phys. J. C* **21** (2001) 33; S. Chekanov *et al.* [ZEUS], *Eur. Phys. J. C* **21** (2001) 443.
- [9] B. B. Abelev *et al.* [ALICE], *Eur. Phys. J. C* **73** (2013) 12, 2662.
- [10] A. Francuz and M. Praszalowicz in preparation.
- [11] A. Bzdak, B. Schenke, P. Tribedy, R. Venugopalan, *Phys. Rev. C* **87** (2013) 064906.
- [12] B. B. Abelev *et al.* [ALICE], *Phys. Lett. B* **727** (2013) 371.
- [13] C. Klein-Bösing, L. McLerran, *Phys. Lett. B* **734** (2014) 282.
- [14] D. Kharzeev, E. Levin and M. Nardi, *Nucl. Phys. A* **747** (2005) 609.
- [15] B. Abelev *et al.* [ALICE], *Phys. Lett. B* **720** (2013) 52.
- [16] J. Adams *et al.* [STAR], *Phys. Rev. Lett.* **91** (2003) 172302.
- [17] C. Adler *et al.* [STAR], *Phys. Rev. Lett.* **89** (2002) 202301.
- [18] S. S. Adler *et al.* [PHENIX], *Phys. Rev. C* **69** (2004) 034910.
- [19] K. Adcox *et al.* [PHENIX], *Phys. Rev. Lett.* **88** (2002) 022301.